Bulgarian Chemical Communications, Volume 56, Special Issue D1 (pp. 77-94) 2024 DOI: 10.34049/bcc.56.D.S1P34

In silico methods for predicting physico-chemical properties and biological activity of newly synthesized esters of Bexarotene

I. R. Iliev*, S. F. Georgieva

Department of Pharmaceutical Chemistry, Faculty of Pharmacy, Medical University of Varna

Received: November 3, 2023; Revised: April 11, 2024

The synthetic retinoid analogue Bexarotene (Targretin®, Ligand Pharmaceuticals Inc.) belongs to a group of compounds called rexinoids. They possess a specific affinity for the retinoid X receptor. The latter plays a role in the regulation of cell growth and differentiation through their ability to regulate transcription. Bexarotene is approved for the treatment of cutaneous T-cell lymphoma (CTCL), both as an oral and dermal dosage form. A total of 4 new Bexarotene esters were synthesized and an *in silico* analysis was performed using the OECD QSAR Toolbox, Molinspiration, PreADME/Tox and SwissADME software. The QSAR Toolbox results show that Bexarotene esters possess high metabolic activity with metabolites similar to those of Bexarotene. Alsom a hydrolysis process is observed making the esters act as prodrugs. According to Lipinski's rule of 5 all four Bexarotene derivatives give 1 violation and therefore have drug-like properties. The Molinspiration and SwissADME software showed affinity of the newly synthesized molecules for nuclear receptors which partly rejects the prodrug theory. After evaluating the pharmacokinetic profile of the esters, it was observed that the molecules present promising intestinal absorption, distribution, metabolism, excretion and toxicity (ADME/T) characteristics. Even though the *in silico* analysis gave promising results, further investigation is needed.

Keywords: pharmacokinetics, bioactivity, esters, prodrugs

INTRODUCTION

Cancer remains a pressing global health concern, accounting for a substantial burden of mortality and morbidity worldwide. According to the World Health Organization, it is estimated that the incidence of cancer will rise to 28.4 million cases by 2040, representing a significant 47% increase from 2020 [1, 2]. In the fight against cancer, the development of novel therapeutic agents and the exploration of their physico-chemical properties and biological activities are crucial for advancing treatment strategies. Bexarotene (Bex), presented in Figure 1, a retinoid X receptor-selective agonist, has exhibited promising potential in the realm of cancer therapy [3].

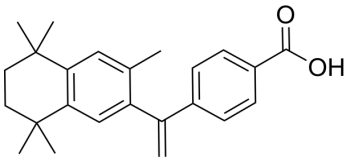

Figure 1. Structure of Bexarotene

The present study focuses on the *in silico* methods employed for predicting the physico-chemical properties and biological activities of newly synthesized esters of Bex. Leveraging computational tools and models, this research aims to streamline the process of identifying and characterizing potential drug candidates with enhanced efficacy and reduced adverse effects. Through the application of advanced computational techniques including quantitative structure-activity relationship (QSAR) analysis, and molecular dynamics simulations, a comprehensive understanding of the molecular interactions and pharmacological profiles of the synthesized esters can be achieved.

The integration of *in silico* approaches offers a holistic perspective on the physico-chemical and pharmacological aspects of the newly synthesized esters of Bex, providing valuable insights for potential applications and further research in cancer therapy. This article explores the use of *in silico* methods to predict the physico-chemical properties and biological activity of these synthesized Bex esters, drawing inspiration from the well-established drug Bex which has shown promise in cancer treatment [4] and potential in addressing central nervous system (CNS) diseases such as Parkinson's, Alzheimer's, and schizophrenia [5].

MATERIALS AND METHODS

For metabolic activation, we employed OECD QSAR Toolbox simulators, including '*In vivo* rat metabolism', 'Rat liver S9 metabolism', and 'Skin metabolism', predicting how the compounds transform in various contexts [6].

* To whom all correspondence should be sent:
E-mail: *i__iliev@abv.bg*

To evaluate toxicity, 'DNA binding by OASIS' and 'Protein binding by OASIS' profilers were used [6].

Molinspiration software (https://molinspiration.com/index.html) [7] calculated crucial molecular properties and predicted bioactivity against drug targets. PreADME/T software (https://preadmet.qsarhub.com/adme/) [8] assessed pharmacokinetic parameters and SwissADME software (https://www.swissadme.ch/) [9] aided in target prediction and understanding potential biological interactions.

The *in silico* analysis provided insights into the esters' properties, enhancing our understanding of their drug potential.

RESULTS AND DISCUSSION

We synthesized four novel Bex esters (E1, E2, E3, and E4) using methanol, ethanol, propanol, and butanol, respectively, following a classical esterification scheme by employing oxalyl chloride as a key reagent. Choosing primary alcohols—methanol, ethanol, propanol, and butanol—for Bex ester synthesis was driven by their enhanced reactivity and availability. This deliberate selection serves a dual purpose: to ensure controlled esterification and to systematically assess the process before exploring higher molecular mass alcohols. Our step-wise approach aligns with a commitment to methodical experimentation, laying a foundation for potential future studies involving larger alcohols.

The synthesized esters were characterized through various analytical techniques, including thin-layer chromatography (TLC), infrared spectroscopy (IR), and high-performance liquid chromatography (HPLC).

TLC analysis revealed distinct Rf values for Bex and the synthesized esters (0.75, 0.55, 0.64, 0.66, and 0.72) using a mobile phase of hexane:ethyl acetate (1:1). The analysis was carried out on UV-plates DC-Fertigfolien ALUGRAM SIL G/UV254 with a layer thickness of 0.20 mm impregnated with fluorescent indicator UV254. Detection was performed with UV light on a Nahita UV lamp.

Infrared spectra were taken in the range 4000-500 cm^{-1} on a Nicolet iS10 FT-IR spectrometer. The IR spectra displayed a notable shift in the peak associated with bexarotene, moving from 1673 cm^{-1} to 1717 cm^{-1}, indicative of the formation of the ester functional group.

Furthermore, HPLC was employed for a detailed characterization, utilizing a Thermo Scientific High Performance Liquid Chromatography (HPLC) apparatus model Spectra SYSTEM HPLC with manual injector, UV-VIS detector model Spectra SYSTEM UV2000 and fluorescence detector model Spectra SYSTEM FL3000. A Synergi 4u Hydro – RP 80A (250 × 4.00 mm) column protected with a Synergi 4u Hydro – RP 80A (250 × 4.00 mm) precolumn was used for the analysis. System control, data acquisition and analysis were performed using ChromQuest chromatographic data software, version 4.2.34. The following conditions were used: mobile phase composed of 60:40 methanol:acetonitrile ratio, flow rate set at 1.3 ml/min, UV detection at 260 nm, chromatographic column temperature of 40 °C, manual injector temperature of 25 °C, and sample volume for analysis set at 20.0 µl. The analysis was performed in isocratic mode, maintaining these conditions throughout a total duration of 15 minutes. The retention times for Bex and the esters were recorded as 5.052, 3.482, 3.752, 4.12, and 4.572 minutes, respectively.

OECD QSAR Toolbox

Our study delved into the metabolic potential of Bex and newly synthesized esters. These esters were created to broaden our investigation and understand their metabolic characteristics compared to the parent compound. Utilizing QSAR models, we examined their metabolic activation, physicochemical properties and factors influencing biological activity. Our research emphasized on assessing not only the parent compound but also the potential for altered biological activity through active metabolites and interactions with DNA and proteins, key considerations for evaluating safety.

Additionally, a mathematical model helped us analyze Bex's metabolic behavior and its physicochemical attributes. The results indicated that neither Bex nor its esters exhibited *in silico* binding to DNA or proteins, suggesting no mutagenic or genotoxic risks. The esters share an identical safety profile with Bex.

In vivo rat metabolism simulator

The study investigated Bex's metabolic activity using the *In vivo* rat metabolism simulator, identifying physicochemical properties influencing its biological activity. Results showed overlapping metabolites between Bex and its esters, due to hydrolysis, suggesting prodrug potential for the esters after oral administration.

These findings are detailed in Tables 1 to 5, presented in the appendix, showcasing metabolites for Bex and esters E1, E2, E3, and E4. Diverse ester metabolites, particularly in larger esters, were observed before hydrolysis, along with alcohol

metabolites, raising concerns about their pharmacological and toxicological effects.

The extensive range of possible metabolites raises concerns about their pharmacological and toxicological effects, emphasizing the need for additional studies to comprehensively assess the biological activity of these metabolites.

We characterized the newly obtained Bex derivatives, focusing on their potential to form active metabolites and interact with DNA and proteins. Both Bex and its esters exhibit the ability to form metabolites that can bind to DNA and proteins, raising concerns about genotoxicity and cellular disruption.

Bex yields 11 metabolites, with none binding to DNA but four binding to proteins. Conversely, the methyl ester (E1) produces 32 metabolites, with five binding to DNA and 15 to proteins. The ethyl ester (E2) generates 28 metabolites, including six binding to DNA and 14 to proteins. The propyl ester (E3) results in 32 metabolites, with four binding to DNA and 15 to proteins. Notably, the butyl ester (E4) is the most metabolically active, with 49 metabolites, seven binding to DNA, and 22 to proteins.

These interactions involve S_N2 reactions for DNA binding and mechanisms like Schiff base formation, nucleophilic addition, and S_N2 reactions for protein binding. For detailed information on binding abilities, refer to Tables 6 and 7, presented in the appendix. Ester E4 stands out as the most metabolically active, producing the highest number of metabolites binding to both DNA and proteins.

Rat liver S9 metabolism simulator

Investigating metabolism using the liver S9 fraction is essential due to its potential to create unique metabolites not seen in *in vivo* liver simulations. Tables 8 to 12, included in the appendix, show metabolites from liver S9 metabolism simulations of Bex and its esters (E1, E2, E3, and E4). Bex generates five metabolites, while esters produce more, with E1 yielding 12, and E2, E3, and E4 each producing 14 metabolites. This suggests that Bex esters might function as prodrugs since they hydrolyze into Bex and precursor alcohols, as seen in Tables 8 to 12, detailed in the appendix.

The study also assessed the potential for DNA and protein binding of metabolites generated in the liver S9 metabolism simulator for Bex and its esters (E1, E2, E3, and E4), as detailed in Table 13, attached in the appendix.

The analysis revealed that both Bex and its esters can form metabolites binding to proteins but not to DNA. This protein binding could potentially disrupt cellular functions or indirectly lead to damage. Notably, none of the metabolites from the rat liver S9 metabolism simulation of Bex and its esters exhibited binding to DNA. Bex produced five metabolites, with three unable to bind to DNA, while two could bind to proteins through nucleophilic addition.

In the case of the E1 ester, eight metabolites did not bind to proteins, while the remaining four exhibited binding through nucleophilic addition. Regarding E2, E3, and E4 esters, nine metabolites showed no binding to proteins, one could bind through Schiff base formation, and four could bind through nucleophilic addition. Importantly, E2, E3, and E4 esters displayed the highest metabolic activity, resulting in more metabolites capable of binding to proteins.

Skin metabolism simulator

Bex is primarily used as a 1% gel for treating Cutaneous T-Cell Lymphoma (CTCL), making it essential to investigate the potential skin metabolism of newly synthesized Bex analogues.

The analysis assessed skin metabolism of Bex and its esters (E1, E2, E3, and E4), as detailed in Table 14, presented within the appendix.

Results indicate that during skin metabolism simulations, Bex generates one metabolite, while its esters each produce four metabolites, with a common metabolite (number 1) across all. Additionally, a hydrolysis process releases Bex (metabolite number 4) and the ester synthesis alcohol. This supports the potential use of Bex esters as prodrugs, aligning with QSAR Toolbox findings.

The study also assessed the potential for DNA and protein binding of metabolites generated in the skin metabolism simulator for Bex and its esters.

Results suggest that both Bex and its esters produce metabolites lacking the ability to bind to DNA or proteins due to their structural properties.

Molinspiration Cheminformatics software

Ideal drug molecules must adhere to Lipinski's rule, which defines specific physicochemical properties for oral bioavailability. Using Molinspiration software, Bex and its esters were evaluated, and they all violated only one rule as seen in Table 15, found in the appendix. This suggests good pharmacokinetic properties and oral bioavailability.

Drug-likeness involves complex molecular properties that impact a molecule's behavior in the body. Using Molinspiration software, it's evident that Bex is highly biologically active, as seen in Table 16 in the appendix. While the esters also

exhibit activity against receptors and enzymes, they may not strictly qualify as prodrugs. However, their activity could enhance the drug's effectiveness. Administering Bex as an ester prodrug at lower doses and less frequently may improve patient compliance.

PreADME/Tox software

Predicting the pharmacokinetic and toxicological profile of molecules is essential in drug development, saving time, cost, and unnecessary animal testing. The results of the *in silico* analysis assessed the absorption, distribution, metabolism, excretion, and toxicity of newly synthesized molecules and is presented in Table 17, included in the appendix.

When considering absorption and distribution, the compounds demonstrated remarkable intestinal absorption, an essential factor in oral drug administration, and an average cellular permeability increasing with molecular mass. Additionally, they exhibited a strong affinity for plasma proteins, which plays a critical role in drug distribution within the body. Among these compounds, Bex esters, unlike Bex, exhibited promising degree of absorption through the blood-brain barrier, hinting at their potential utility in the treatment of central nervous system (CNS) diseases such as Alzheimer's and Parkinson's and schizophrenia.

Regarding metabolism, all compounds were found to inhibit CYP2C9, and only Bex didn't inhibit CYP3A4. This suggests potential drug interactions and emphasizes caution when co-administering these compounds with others metabolized by the same enzymes.

In the context of excretion, the compounds exhibited low permeability in MDCK cell permeability assays, indicating prolonged renal excretion.

Turning to toxicity, the analysis raised concerns about mutagenicity, as all tested compounds displayed mutagenic effects, necessitating further *in vitro* and *in vivo* investigations to meticulously weigh the therapeutic advantages against potential risks. Encouragingly, only E1 exhibited carcinogenic activity in rat models, indicating a significant level of safety for compounds E2, E3, and E4. Moreover, the risk of cardiotoxicity, as indicated by inhibition of the hERG gene, was moderate for the assessed compounds.

In sum, the *in silico* evaluation provided a comprehensive ADME/T profile for the newly synthesized esters. Of particular note were the promising characteristics exhibited by E2, E3, and E4, rendering them potential candidates for CNS antineoplastic treatments.

SwissADME Target Prediction

In the target prediction analysis using SwissADME software for Bex and its newly synthesized esters, it was observed that esterification of Bex substantially reduces the probability of binding to RAR or RXR receptors, with this reduction becoming more pronounced as the ester size increases. This observation aligns with the data presented in Table 18 in the appendix. SwissTargetPrediction reaffirms the findings obtained from Molinspiration software.

Additionally, the analysis reveals a wide range of G-protein coupled receptors and enzymes that Bex and its esters can potentially interact with, supporting the results presented in Table 16 in the appendix. These interactions highlight the diverse pharmacological potential of these compounds in various biological systems. The compounds E1, E2, E4, and Bex exhibit interactions with various enzymes and receptors, hinting at potential central nervous system (CNS) effects. These include receptors associated with circadian rhythm regulation (Melatonin Receptor 1A and 1B), cognitive functions (Neuronal Acetylcholine Receptor Protein Alpha-7 Subunit), mood regulation (Serotonin 5a Receptor), stress responses and attention (Alpha-2b Adrenergic Receptor), Alzheimer's disease (Gamma-Secretase), sleep disorders (Adenosine A3 Receptor), synaptic plasticity and neurological disorders, such as schizophrenia (Metabotropic Glutamate Receptor 1), inhibitory signaling (Glycine Transporter 1), pain modulation (Mu Opioid Receptor), and wakefulness (Histamine H3 Receptor).

While these interactions suggest potential CNS effects, empirical studies are needed to validate these predictions. Understanding the precise mechanisms of action and clinical utility in CNS-related disorders requires further research and experimental validation.

CONCLUSION

In conclusion, our research harnessed the power of advanced metabolism simulator models to delve deep into the pharmacokinetic and toxicological aspects of newly synthesized Bex esters. Through a comprehensive analysis employing the *in vivo* rat metabolism simulator, liver S9 metabolism simulator, and skin metabolism simulator, we gained critical insights into how these compounds undergo transformations within the body.

The outcomes of our simulations underscore the promising potential of Bex esters as prodrugs, with

hydrolysis leading to the release of Bex and precursor alcohols. Particularly striking was the observation that the esters produced a greater number of metabolites compared to Bex alone, emphasizing their versatility in metabolic pathways.

Our research underscores the indispensable role of metabolism simulator models in the drug development process, offering invaluable insights that could shape the future of innovative therapies. While our study represents significant progress, the journey from synthesis to clinical application remains dynamic and full of potential, promising advancements in medical care.

Moreover, our study shed light on the pharmacokinetic properties of these esters, revealing their excellent intestinal absorption rates. Of special note are compounds E2, E3, and E4, which exhibited promising profiles for potential CNS antineoplastic applications.

However, it is crucial to acknowledge the concerns raised about mutagenicity, underlining the necessity for further *in vitro* and *in vivo* investigations to comprehensively evaluate the therapeutic benefits and associated risks.

The SwissTargetPrediction analysis expanded our horizons, revealing a decreasing likelihood of binding to RAR or RXR receptors with increasing ester size, a phenomenon confirmed by the Molinspiration software. Furthermore, the wide array of interactions observed with G-protein coupled receptors and enzymes hints at the diverse biological activities these esters might exhibit.

Notably, the tantalizing potential of these compounds in CNS applications adds an intriguing dimension to their therapeutic prospects. While further studies are imperative to validate these CNS effects, our findings provide a solid foundation for future investigations into the utilization of these esters in treating CNS disorders, such as Parkinson's, Alzheimer's, and schizophrenia.

In summary, our research findings collectively contribute to the characterization of these esters and their potential as promising drug candidates, not only in the realm of oncology but also in the exciting domain of CNS therapeutics. To unlock their full therapeutic potential in various medical applications, further studies, encompassing both *in vitro* and *in vivo* investigations, are warranted.

Acknowledgement: *This work was funded by Fund 'Nauka' at the Medical University of Varna, Bulgaria, through Project No. 20008, 'Study of the toxicity of hydrazones of Bex using in vitro and in vivo models', Competition-Based Session for Scientific Research Projects, 2021.*

REFERENCES

1. M. Georgieva, D. Tzankova, E. Mateev, B. Angelov, M. Kondeva-Burdina, G. Momekov, V. Tzankova, A. Zlatkov, *Anti-cancer Agents Medicinal Chemistry*, **23** (3), 346 (2023). doi: 10.2174/1871520622666220701114306.
2. International Agency for Research on Cancer. Global Cancer Statistics 2020: GLOBOCAN Estimates of Incidence and Mortality Worldwide for 36 Cancers in 185 Countries. CA: *A Cancer Journal for Clinicians*, 2020.
3. F. Cayrol, M. V. Revuelta, M. Debernardi, A. Paulazo, J. M. Phillip, N. Zamponi, H. Sterle, M. C. Díaz Flaqué, C. Magro, R. Marullo, E. Mulvey, J. Ruan, G. A. Cremaschi, L. Cerchietti. *Mol Cancer Ther.* **21** (9), 1485 (2022) https://doi.org/10.1158/1535-7163.MCT-22-0093.
4. P. Collins, C. Jones, S. Choudhury, L. Damelin. Tracing the Journey of Bexarotene from Drug Discovery to the Clinic: An Historical Perspective. *International Journal of Molecular Sciences*. **20** (9), 2159 (2019) doi:10.3390/ijms20092159.
5. Y. Liu, P. Wang, G. Jin, P. Shi, Y. Zhao, J. Guo, Y. Yin, Q. Shao, P. Li, P. Yang. *Ageing Research Reviews*, **90**, page (2023), 102021, ISSN 1568-1637, https://doi.org/10.1016/j.arr.2023.102021.
6. U.S. Environmental Protection Agency. (2021). QSAR Toolbox. https://www.epa.gov/chemical-research/qsar-toolbox
7. Molinspiration Cheminformatic. (n.d.). Molinspiration Property Calculation. https://www.molinspiration.com/
8. PreADME/T. (n.d.). PreADME/T. https://preadmet.qsarhub.com/
9. A. Daina, O. Michielin, V. Zoete. SwissADME: A free web tool to evaluate pharmacokinetics, drug-likeness and medicinal chemistry friendliness of small molecules. *Scientific Reports*, **7** (1) 42717 (2017). doi:10.1038/srep42717 http://www.swissadme.ch/index.php

APPENDIX

Table 1. Numbers and structure of predicted metabolites of Bex obtained after *in vivo* rat metabolism simulator.

1	2	3	4
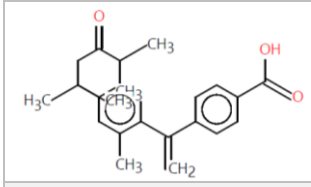	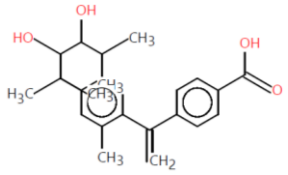	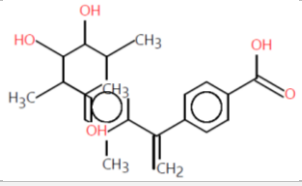	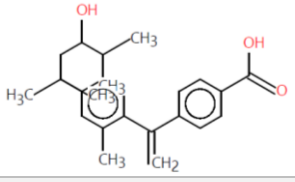
5	**6**	**7**	**8**
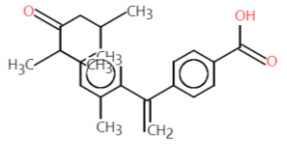	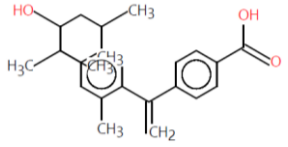	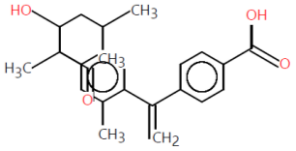	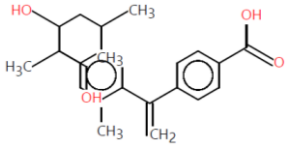
9	**10**	**11**	
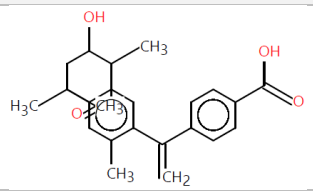	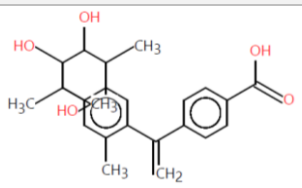	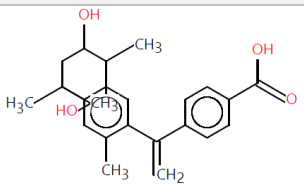	

Table 2. Numbers and structure of predicted metabolites of compound E1 obtained after *in vivo* rat metabolism simulator.

1	2	3	4
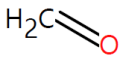	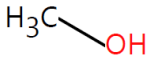	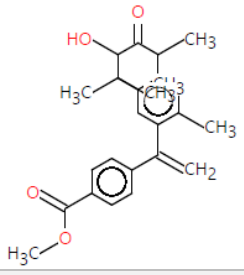	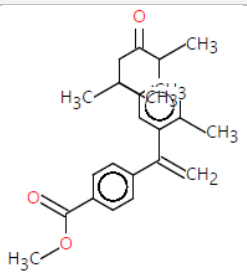
5	**6**	**7**	**8**
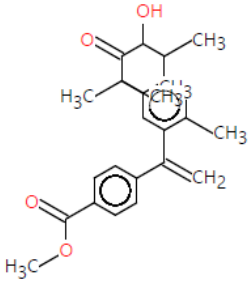	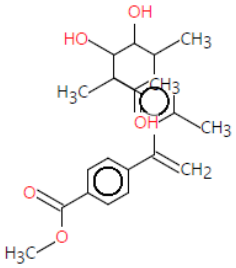	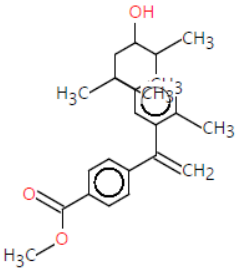	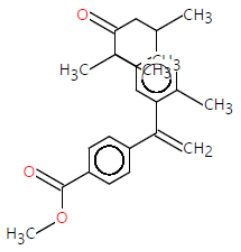
9	**10**	**11**	**12**
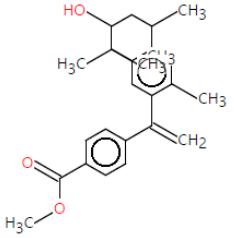	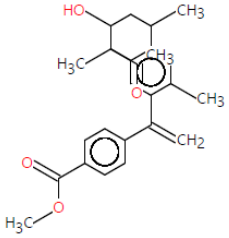	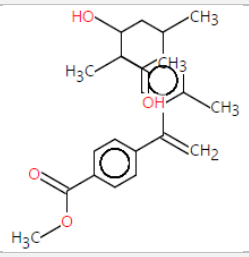	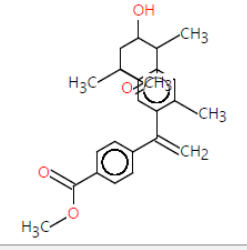

13	14	15	16
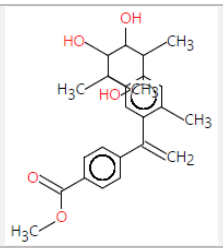	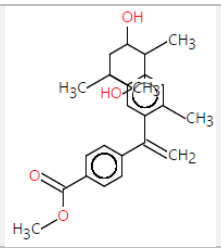	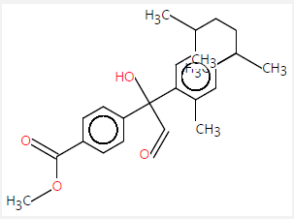	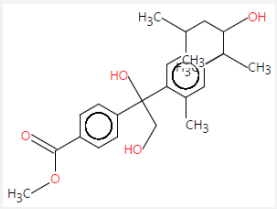
17	**18**	**19**	**20**
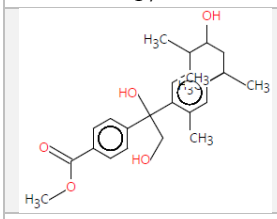	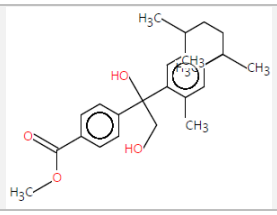	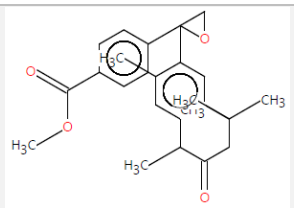	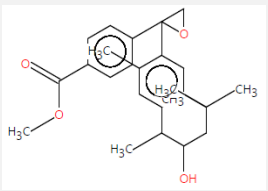
21	**22**	**23**	**24**
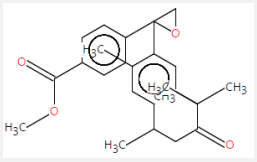	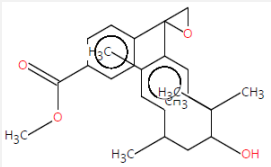	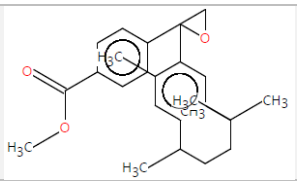	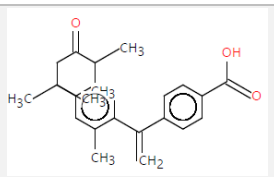
25	**26**	**27**	**28**
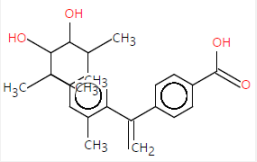	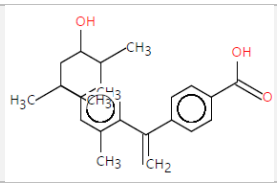	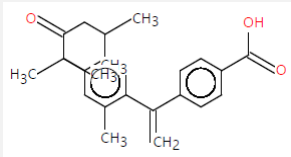	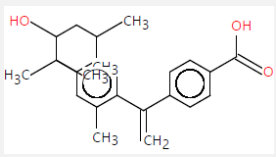
29	**30**	**31**	**32**
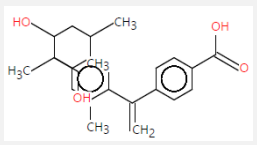	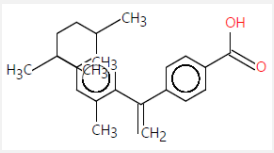	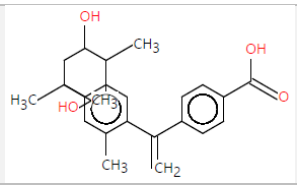	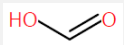

Table 3. Numbers and structure of predicted metabolites of compound E2 obtained after *in vivo* rat metabolism simulator.

1	2	3	4
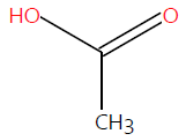	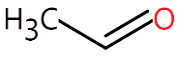	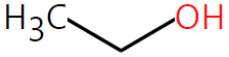	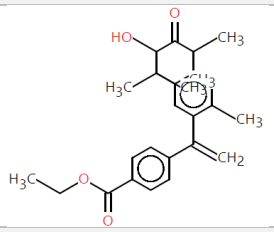
5	**6**	**7**	**8**
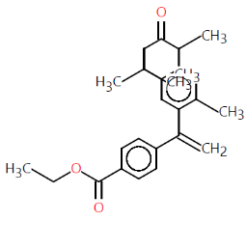	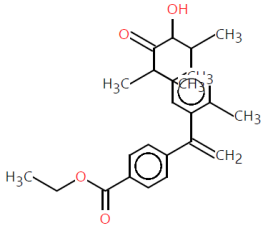	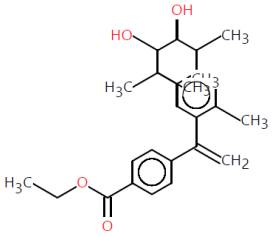	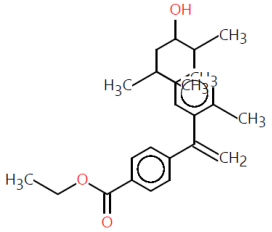

9	10	11	12
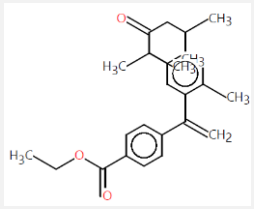	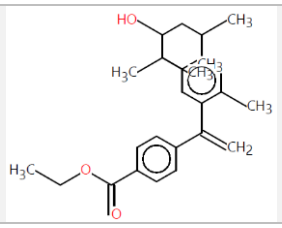	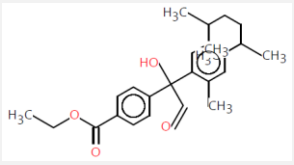	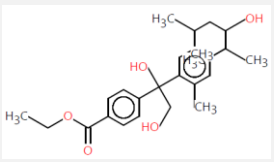
13	14	15	16
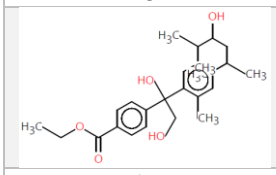	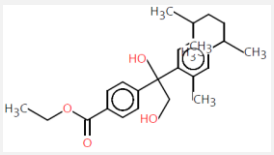	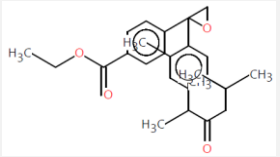	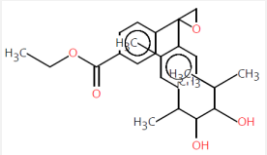
17	18	19	20
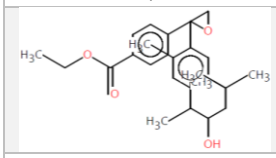	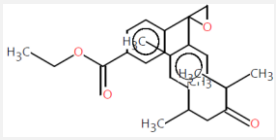	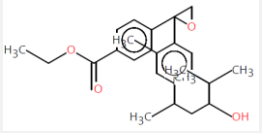	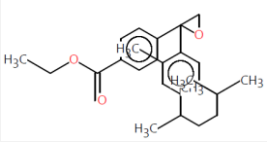
21	22	23	24
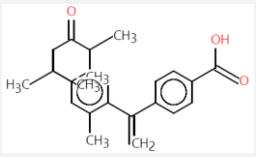	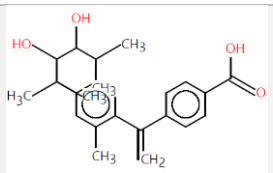	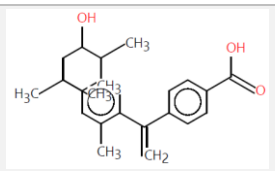	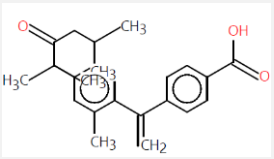
25	26	27	28
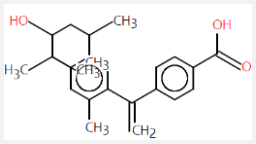	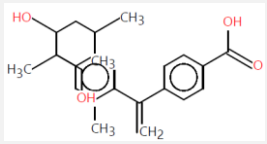	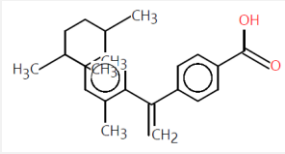	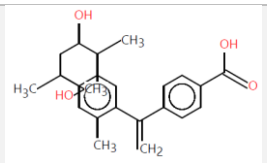

Table 4. Numbers and structure of predicted metabolites of compound E3 obtained after *in vivo* rat metabolism simulator.

1	2	3	4
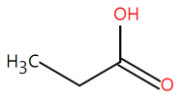	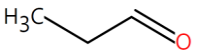	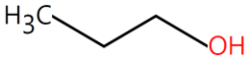	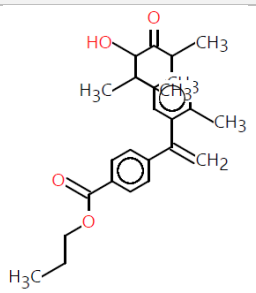
5	6	7	8
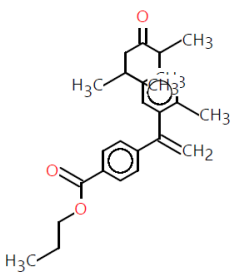	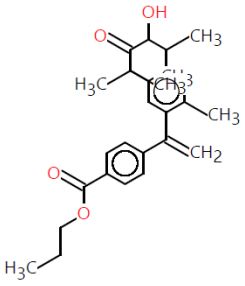	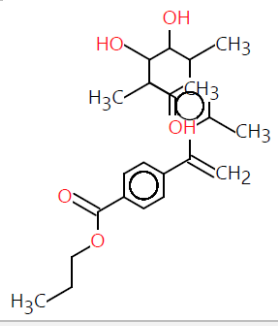	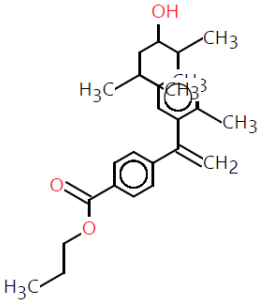

9	10	11	12
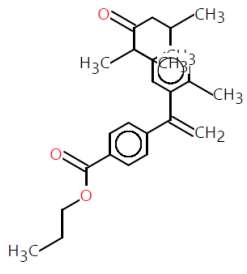	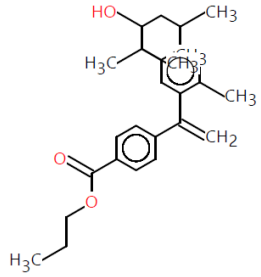	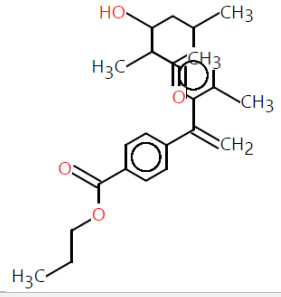	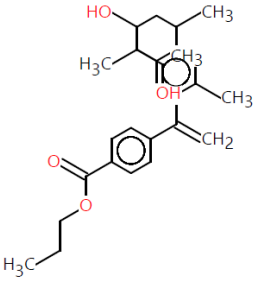
13	14	15	16
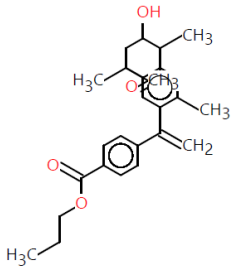	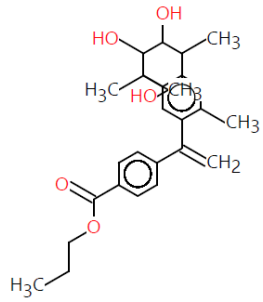	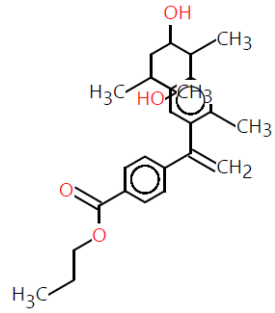	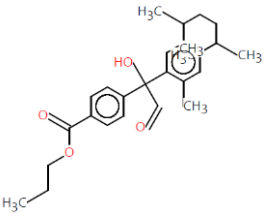
17	18	19	20
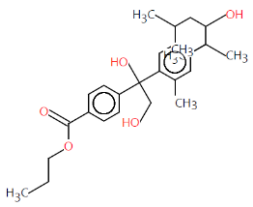	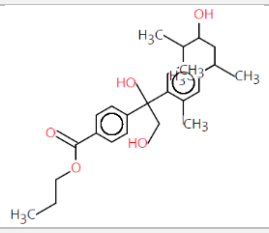	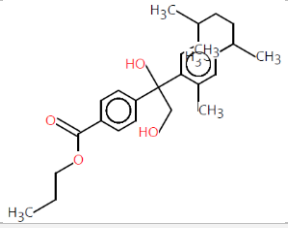	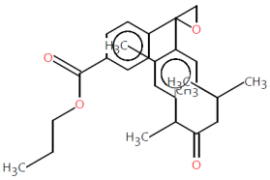
21	22	23	24
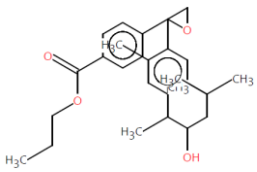	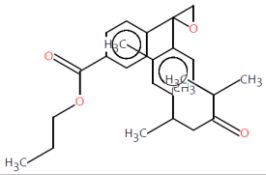	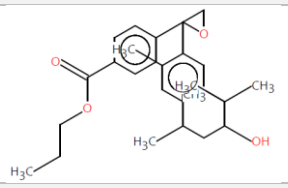	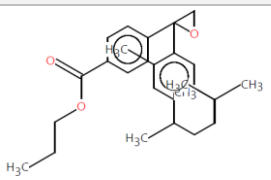
25	26	27	28
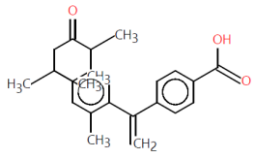	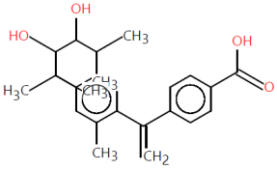	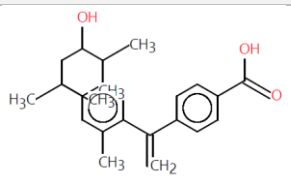	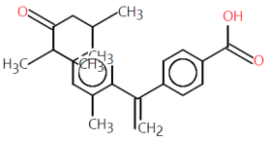
29	30	31	32
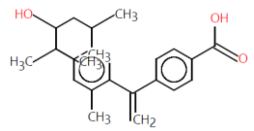	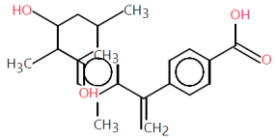	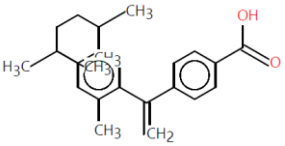	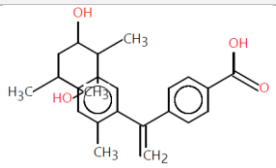

Table 5. Numbers and structure of predicted metabolites of compound E4 obtained after *in vivo* rat metabolism simulator.

1	2	3	4
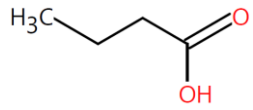	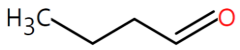	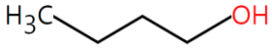	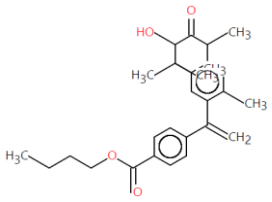
5	6	7	8
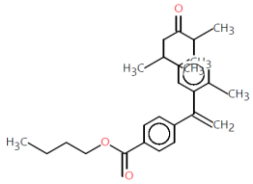	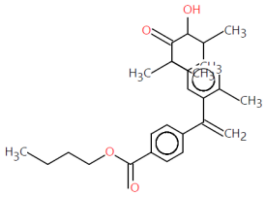	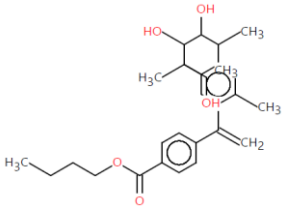	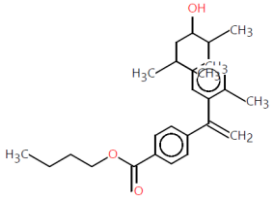
9	10	11	12
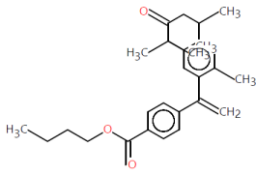	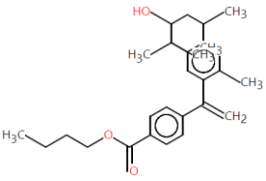	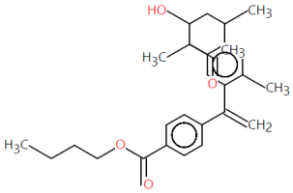	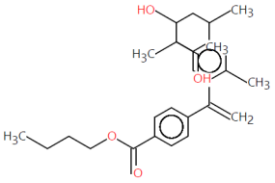
13	14	15	16
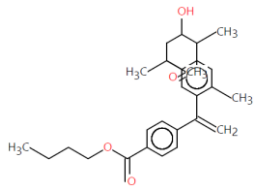	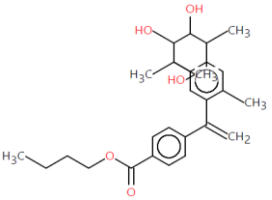	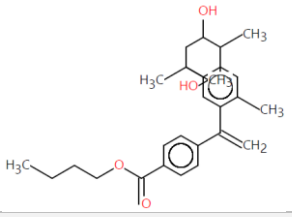	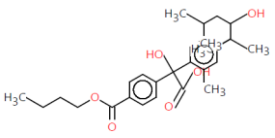
17	18	19	20
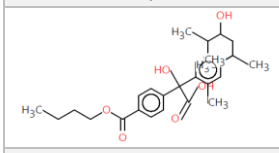	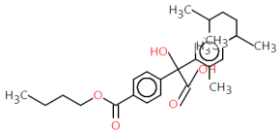	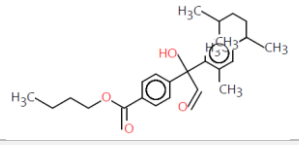	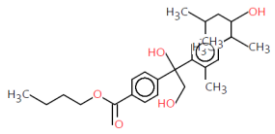
21	22	23	24
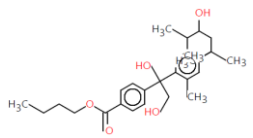	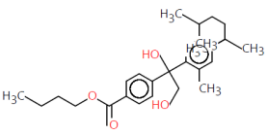	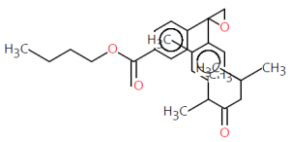	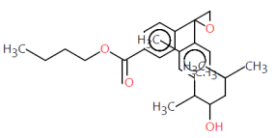
25	26	27	28
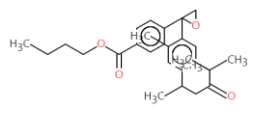	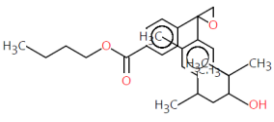	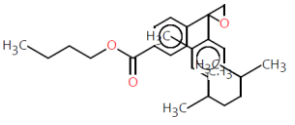	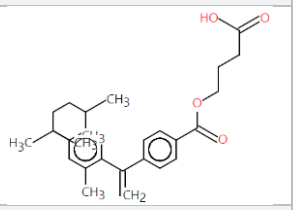
29	30	31	32
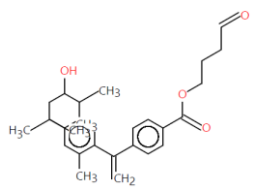	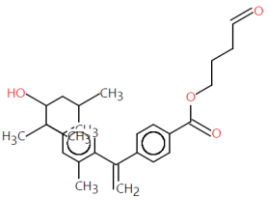	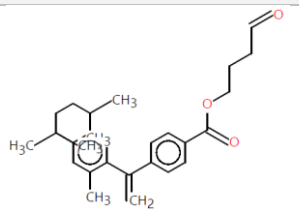	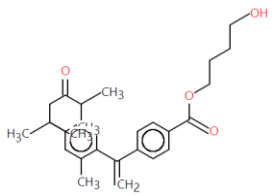

33	34	35	36
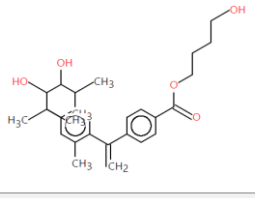	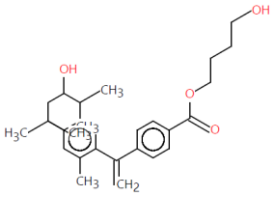	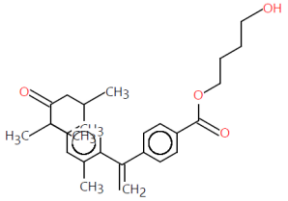	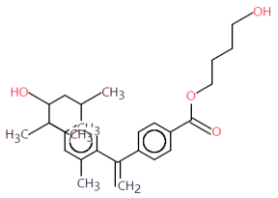
37	**38**	**39**	**40**
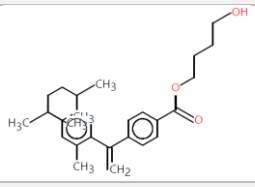	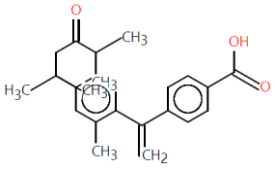	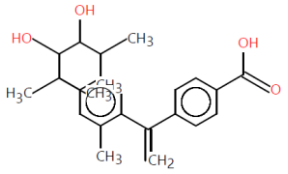	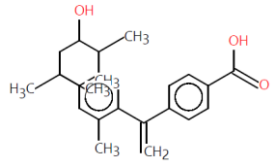
41	**42**	**43**	**44**
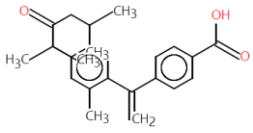	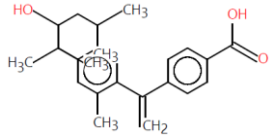	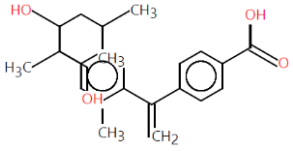	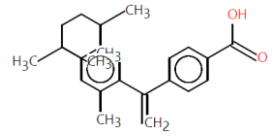
45	**46**	**47**	**48**
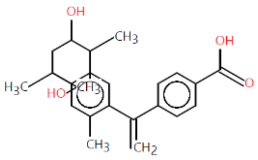	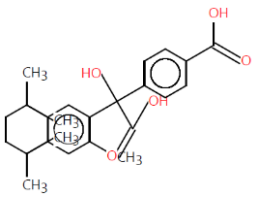	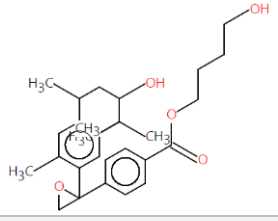	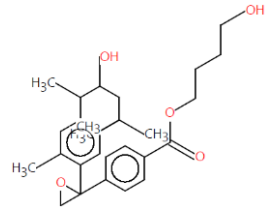
49			
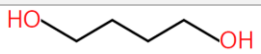			

Table 6. Binding of Bex and Bex esters metabolites to DNA.

DNA binding	*Structural alert*	*No alert found*	*Epoxides, Aziridines, Thiiranes and Oxetanes*
	Mechanistil alert	-	*Alkylation, direct acting epoxides and related*
	Mechanistic domain	-	S_N2
Metabolite №	*Bex*	1-11	-
	E1	1-18, 24-32	19-23
	E2	1-14, 21-28	15-20
	E3	1-19, 25-32	20-24
	E4	1-22, 28-46, 49	23-27, 47, 48

Table 7. Binding of Bex and Bex esters metabolites to proteins.

Protein binding	*Structural alert*	*No alert found*	*Aldehydes*	*Ketones*	*Epoxides, Aziridines and Sulfuranes*
	Mechanistic alert	-	*Schiff base formation with carbonyl compounds*	*Addition to carbon-hetero double bond*	*Ring opening S_N2 reaction*
	Mechanistic domain	-	*Schiff base formation*	*Nucleophilic addition*	S_N2
Metabolite	*Bex*	2-4, 6, 8, 10, 11	7, 9	1, 5	-

	E1	2, 6, 7, 9, 11, 13, 14, 16-18, 25, 26, 28-32	1, 10, 12, 15	3-5, 8, 19, 21, 24, 27	19-23
	E2	1, 3, 7, 8, 10, 12-14, 22, 23, 25-28	2, 11	4-6, 9, 15, 18, 21, 24	15-20
	E3	1, 3, 7, 8, 10, 12, 14, 15, 17-19, 26, 27, 29-32	2, 11, 13, 16	4-6, 9, 20, 22, 25, 28	20-24
	E4	1, 3, 7, 8, 10, 12, 14-18, 20-22, 28, 33, 34, 36, 37, 39, 40, 42-46, 49	2, 11, 13, 19, 29-31	4-6, 9, 23, 25, 32, 35, 38, 41	23-27, 47, 48

Table 8. Numbers and structure of predicted metabolites of Bex obtained after rat liver S9 metabolism simulator.

1	2	3	4
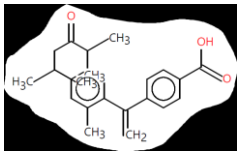	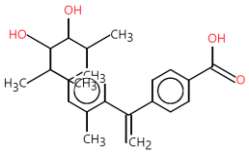	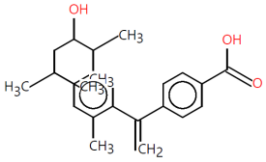	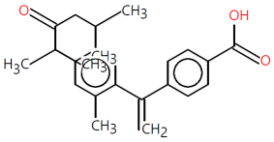
5			
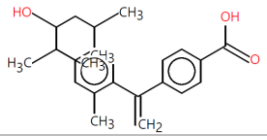			

Table 9. Numbers and structure of predicted metabolites of compound E1 obtained after rat liver S9 metabolism simulator.

1	2	3	4
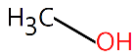	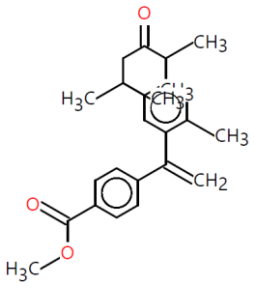	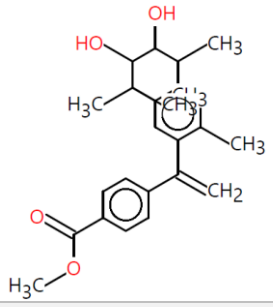	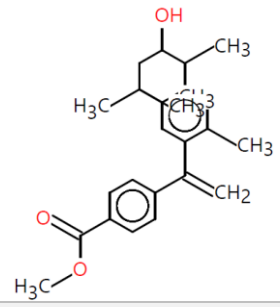
5	6	7	8
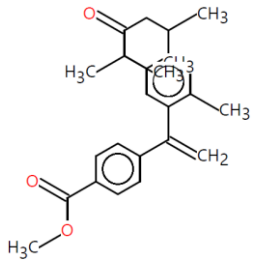	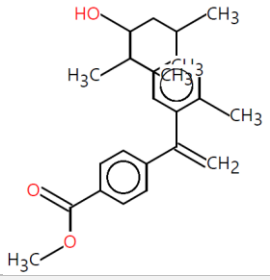	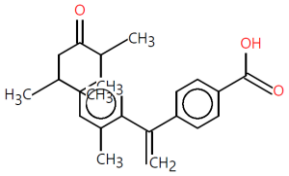	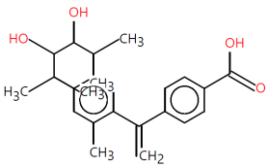
9	10	11	12
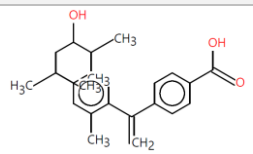	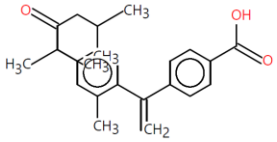	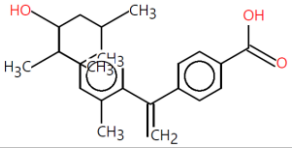	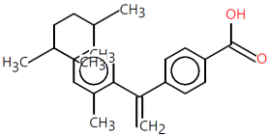

Table 10. Numbers and structure of predicted metabolites of compound E2 obtained after rat liver S9 metabolism simulator.

1	2	3	4
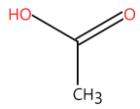	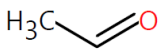	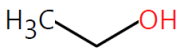	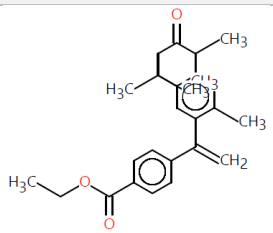
5	**6**	**7**	**8**
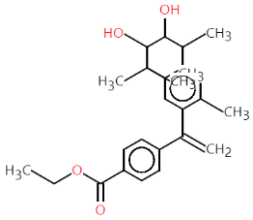	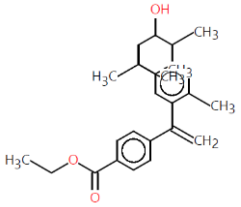	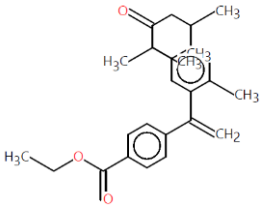	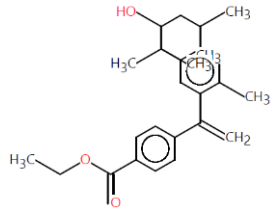
9	**10**	**11**	**12**
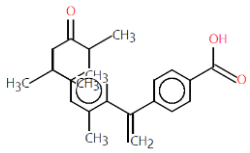	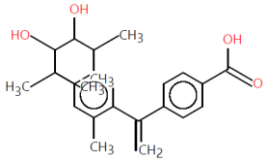	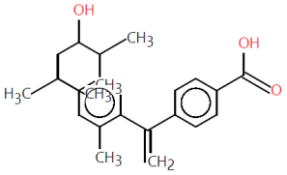	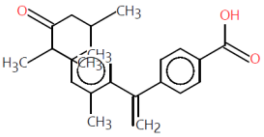
13		**14**	
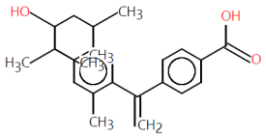		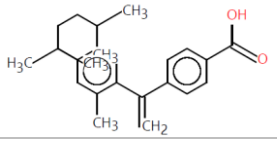	

Table 11. Numbers and structure of predicted metabolites of compound E3 obtained after rat liver S9 metabolism simulator.

1	2	3	4
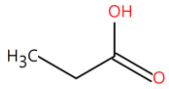	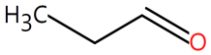	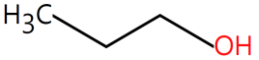	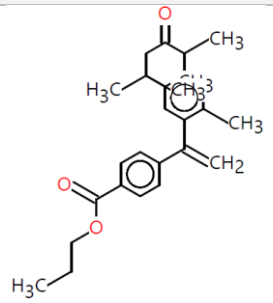
5	**6**	**7**	**8**
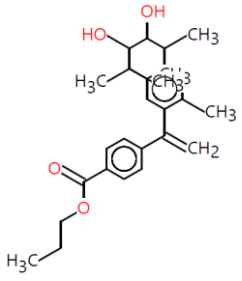	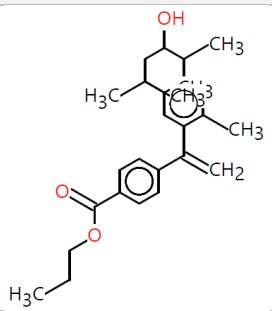	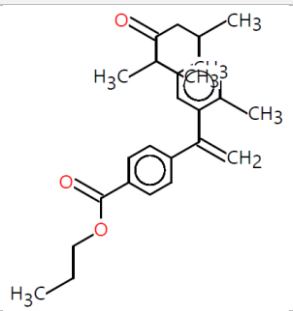	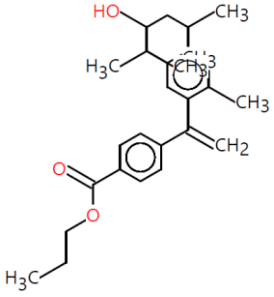

9	10	11	12
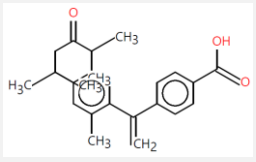	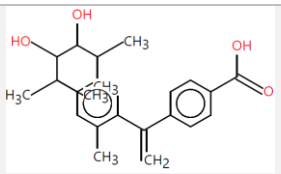	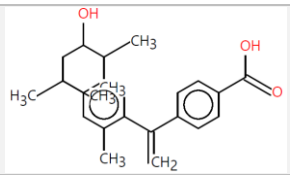	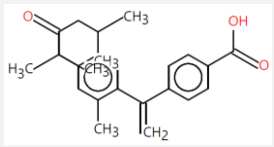
13		14	
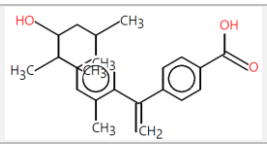		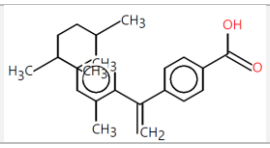	

Table 12. Numbers and structure of predicted metabolites of compound E4 obtained after rat liver S9 metabolism simulator.

1	2	3	4
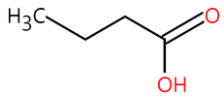	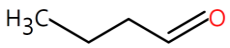	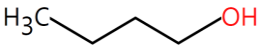	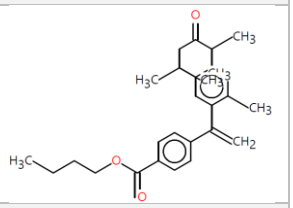
5	6	7	8
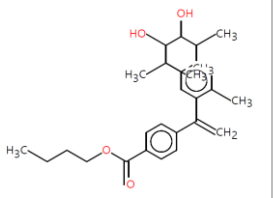	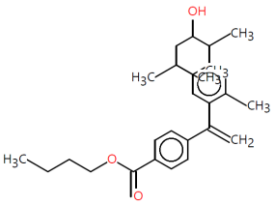	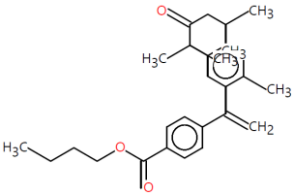	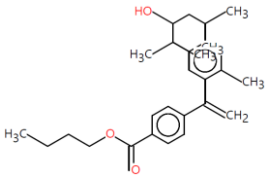
9	10	11	12
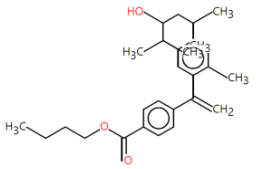	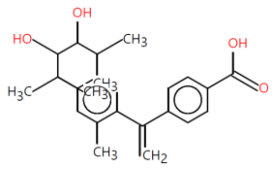	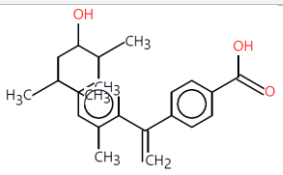	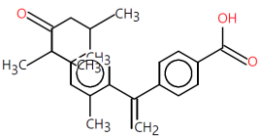
13		14	
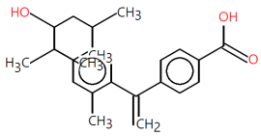		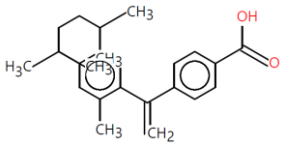	

Table 13. Binding of Bex and Bex esters metabolites to DNA and proteins.

DNA binding	*Structural alert*	*No alert found*	Protein binding	*Structural alert*	*No alert found*	*Aldehydes*	*Ketones*
	Mechanistic domain	-		*Mechanistic domain*	-	*Schiff base formation with carbonyl compounds*	*Addition to carbon-hetero double bonds*
	Mechanistic domain	-		*Mechanistic domain*	-	*Schiff base formation*	*Nuclephilic addition*
Metabolite	*Bex*	*1-5*	*Metabolite*	*Bex*	2, 3, 5	-	1, 4
	E1	*1-12*		*E1*	1, 3, 4, 6, 8, 9, 11, 12	-	2, 5, 7, 10
	E2	*1-14*		*E2*	1, 3, 5, 6, 8, 10, 11, 13, 14	2	4, 7, 9, 12

	E3	*1-14*		*E3*	1, 3, 5, 6, 8, 10, 11, 13, 14	2	4, 7, 9, 12
	E4	*1-14*		*E4*	1, 3, 5, 6, 8, 10, 11, 13, 14	2	4, 7, 9, 12

Table 14. Numbers and structure of predicted metabolites of Bex and its esters E1, E2, E3 and E4 obtained after skin metabolism simulator.

№	1	2	3	4
Bex	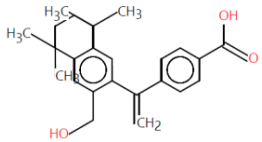	-	-	-
E1	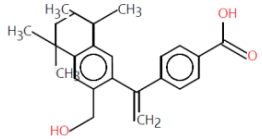	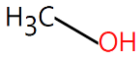	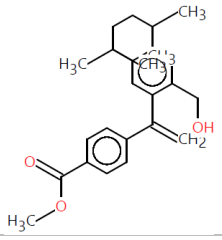	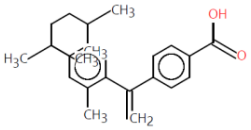
E2	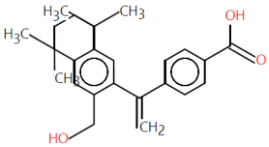	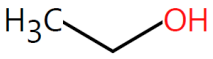	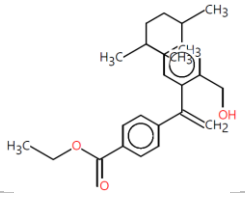	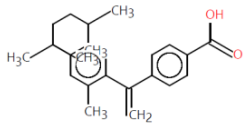
E3	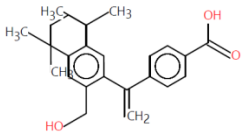	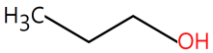	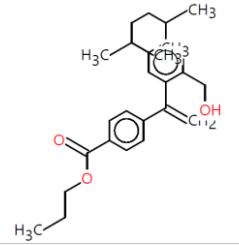	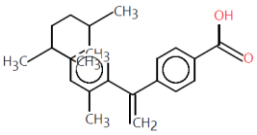
E4	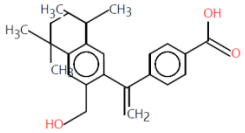	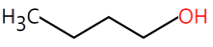	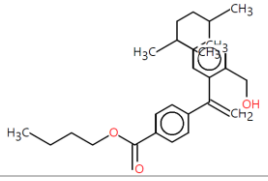	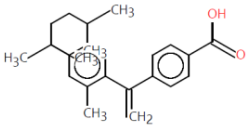

Table 15. Pharmacokinetic parameters of Bex and newly synthesized Bex esters obtained using Molinspiration software.

Property	Bex	E1	E2	E3	E4
miLogP	6.81	7.07	7.44	7.95	8.41
TPSA	37.30	26.30	26.30	26.30	26.30
Molecular mass	348.49	362.51	376.54	390.57	404.59
Number of H- acceptors	2	2	2	2	2
Number of H- donors	1	0	0	0	0
Number of violations	1	1	1	1	1
Number of rotatable bonds	3	4	5	6	7
Molecular volume	348.76	366.29	383.09	399.89	416.69

Table 16. Bioactivity results of Bex and newly synthesized Bex esters obtained using Molinspiration software.

Property	*Bex*	*E1*	*E2*	*E3*	*E4*
GPCR ligand	0.47	0.32	0.28	0.30	0.33
Ion channel modulator	0.14	0,04	0.06	0.05	0.07
Kinase inhibitor	0.01	-0.06	-0.11	-0.09	-0.07
Nuclear receptor lignad	0.92	0.71	0.70	0.68	0.68
Protease inhibitor	0.02	-0.10	-0.13	-0.11	-0.07
Enzyme inhibitor	0.39	0.24	0.20	0.23	0.25

Table 17. Pharmacokinetic and toxicological parameters of Bex and newly synthesized Bex esters using PredADME/T software.

	ADME/T parameters	Bex	E1	E2	E3	E4
A	*HIA*	97.93	100	100	100	100
	Caco-2	22.220	27.559	42.081	43.436	44.676
	Skin permeability	-0.7892	-0.7898	-0.7696	-0.7324	-0.7089
D	*PPB*	100	100	100	100	100
	BBB	1.8619	9.2775	11.216	13.846	15.833
M	*CYP3A4 inhibitor*	-	Inhibitor	Inhibitor	Inhibitor	Inhibitor
	CYP3A4 substrate	Substrate	Substrate	Substrate	Substrate	Substrate
	CYP2C19 inhibitor	-	-	-	-	-
	CYP2C9 inhibitor	Inhibitor	Inhibitor	Inhibitor	Inhibitor	Inhibitor
	CYP2D6 inhibitor	-	-	-	-	-
	CYP2D6 substrate	-	-	-	-	-
E	*MDCK*	0.077539*	0.073390*	0.065640*	0.098970*	0.092798*
T	*Ames test*	+	+	+	+	+
	Carcinogenicity in rats	-	+	-	-	-
	Carcinogenicity in mice	-	-	-	-	-
	hERG Inhibition	Medium	Medium	Medium	Medium	Medium

Human intestinal absorption (HIA): Low absorption 0.00 – 20.00 %; Moderate absorption 20.00 – 70.00 %; Excellent absorption 70.00 – 100.00 %;

Caco-2 cell permeability: High permeability > 70.0 nm/sec; Medium permeability 4.0 - 70.0 nm/sec; Low permeability < 4.0 nm/sec;

Skin permeability: values vary from -3.00 to 6.00;

Plasma Protein Binding (PPB): Strong connection > 90.0%; Weak connection < 90.0

Blood Brain Barrier (BBB): High CNS absorption > 2.00; Intermediate CNS absorption 0.10 ÷ 2.00; Low CNS absorption < 0.10

MDCK: Low permeability < 25.0 nm/sec; Medium permeability 25.0 ÷ 500.0 nm/sec; high permeability > 500.0 nm/sec

Ames test: Positive: mutagenic; Negative: non-mutagenic.

Carcinogenicity: Positive: carcinogenic; Negative: non-carcinogenic.

Table 18. Swiss Target Prediction and predicted probability of binding of Bex and its newly synthesized esters.

Target	Probability, %				
	Bex	E1	E2	E3	E4
Retinoid X receptor beta	100	18.52	15.67	11.32	11.45
Retinoic acid receptor gamma	100	14.53	13.21	11.32	11.45
Retinoid X receptor gamma	100	12.93	13.21	11.32	11.45
Retinoic acid receptor beta	100	14.53	13.21	11.32	11.45
Retinoic acid receptor alpha	100	14.53	13.21	11.32	11.45
Retinoid X receptor alpha	100	12.93	13.21	11.32	11.45

Cytochrome P450 26B1	100	18.52	17.31	12.20	10.62
Cytochrome P450 26A1	11.75	0.00	11.57	0.00	10.62
Nuclear receptor ROR-gamma	10.93	11.33	11.57	0.00	10.62
Prostanoid EP4 receptor	10.93	0.00	0.00	0.00	0.00
Prostanoid EP1 receptor	10.93	0.00	0.00	0.00	0.00
Steroid 5-alpha-reductase 2	10.93	0.00	0.00	0.00	0.00
Peroxisome proliferator-activated receptor alpha	10.93	0.00	0.00	0.00	0.00
Peroxisome proliferator-activated receptor gamma	10.93	0.00	0.00	0.00	0.00
Peroxisome proliferator-activated receptor delta	10.93	0.00	0.00	0.00	0.00
Hepatocyte nuclear factor 4-alpha	10.93	11.33	11.57	0.00	10.62
Arachidonate 5-lipoxygenase	10.93	0.00	0.00	0.00	0.00
Free fatty acid receptor 1	10.93	0.00	0.00	0.00	0.00
Monocarboxylate transporter 1 (by homology)	10.93	0.00	0.00	0.00	0.00
Acyl-CoA desaturase	10.93	0.00	0.00	0.00	0.00
Leukotriene B4 receptor 1	10.93	0.00	0.00	0.00	0.00
G protein-coupled receptor 44	10.93	0.00	0.00	0.00	0.00
Solute carrier family 22 member 12	10.93	0.00	0.00	0.00	0.00
11-beta-hydroxysteroid dehydrogenase 1	10.93	11.33	11.57	0.00	10.62
Prostanoid DP receptor	10.93	0.00	0.00	0.00	0.00
T-cell protein-tyrosine phosphatase	10.93	0.00	0.00	0.00	0.00
p53-binding protein Mdm-2	10.93	0.00	0.00	0.00	0.00
Prostaglandin E synthase 2	10.93	0.00	0.00	0.00	10.62
Transient receptor potential cation channel subfamily M member 8	10.93	0.00	0.00	0.00	0.00
Alpha-2b adrenergic receptor	10.93	0.00	0.00	0.00	0.00
Adenosine A3 receptor	10.93	0.00	0.00	0.00	0.00
Gamma-secretase	10.93	0.00	0.00	0.00	0.00
Thromboxane-A synthase	10.93	0.00	0.00	0.00	0.00
Epoxide hydratase	10.93	11.33	11.57	0.00	0.00
Tyrosine-protein kinase receptor FLT3	0.00	11.33	0.00	0.00	0.00
Vasopressin V2 receptor	0.00	11.33	11.57	0.00	10.62
Cytochrome P450 11B1	0.00	11.33	11.57	0.00	0.00
Cytochrome P450 11B2	0.00	11.33	11.57	0.00	0.00
Cytochrome P450 19A1	0.00	11.33	0.00	0.00	0.00
Cytochrome P450 17A1 (by homology)	0.00	11.33	11.57	0.00	0.00
Metabotropic glutamate receptor 1	0.00	11.33	0.00	0.00	0.00
Glycine transporter 1 (by homology)	0.00	11.33	0.00	0.00	0.00
Histamine H3 receptor	0.00	11.33	11.57	0.00	0.00
P2X purinoceptor 7	0.00	11.33	11.57	0.00	0.00
Voltage-gated calcium channel alpha2/delta subunit 1	0.00	11.33	0.00	0.00	0.00
Melatonin receptor 1A	0.00	11.33	0.00	0.00	10.62
Melatonin receptor 1B	0.00	11.33	0.00	0.00	10.62
Glutaminyl-peptide cyclotransferase	0.00	11.33	0.00	0.00	0.00
Nuclear factor NF-kappa-B p65 subunit	0.00	11.33	11.57	0.00	0.00
Carbonic anhydrase II	0.00	11.33	0.00	0.00	0.00

Carbonic anhydrase VII	0.00	11.33	0.00	0.00	0.00
Carbonic anhydrase XII	0.00	11.33	0.00	0.00	0.00
Carbonic anhydrase XIV	0.00	11.33	0.00	0.00	0.00
Carbonic anhydrase IX	0.00	11.33	0.00	0.00	0.00
Metabotropic glutamate receptor 5 (by homology)	0.00	0.00	11.57	0.00	10.62
C-X-C chemokine receptor type 3	0.00	0.00	11.57	0.00	10.62
Phosphodiesterase 10A	0.00	0.00	11.57	0.00	10.62
Vasopressin V1a receptor	0.00	0.00	11.57	0.00	10.62
Protein farnesyltransferase	0.00	0.00	11.57	0.00	0.00
Geranylgeranyl transferase type I	0.00	0.00	11.57	0.00	0.00
Plasma retinol-binding protein	0.00	0.00	11.57	0.00	0.00
Mu opioid receptor	0.00	0.00	11.57	0.00	0.00
Neuronal acetylcholine receptor protein alpha-7 subunit	0.00	0.00	11.57	0.00	0.00
5-lipoxygenase activating protein	0.00	0.00	11.57	0.00	10.62
Adenosine A2a receptor	0.00	0.00	11.57	0.00	0.00
Dual specificity protein phosphatase 3	0.00	0.00	11.57	0.00	0.00
Tankyrase-1	0.00	0.00	11.57	0.00	0.00
Proteinase-activated receptor 1	0.00	0.00	0.00	0.00	10.62
C-C chemokine receptor type 1	0.00	0.00	0.00	0.00	10.62
Serotonin 5a (5-HT5a) receptor	0.00	0.00	0.00	0.00	10.62
Type-1 angiotensin II receptor (by homology)	0.00	0.00	0.00	0.00	10.62
Phosphodiesterase 7A	0.00	0.00	0.00	0.00	10.62